Formation Mechanism of Micrometer-Sized Carbon Tubes

Chien-Chung Han,* Jyh-Tsung Lee, Reen-Woei Yang, and Chein-Hwa Han†

Department of Chemistry, National Tsing Hua University, Hsinchu, Taiwan, ROC

Received February 16, 2001. Revised Manuscript Received May 11, 2001

Micrometer-sized carbon tubes and their regularly assembled structures can be easily prepared via the pyrolysis of composite fibers consisting of a poly(ethylene terephthalate) (PET) core and a conducting polymer skin layer, such as polypyrrole (PPy). Using this new chemical approach, the diameter, wall thickness, and length of carbon tubes can be effectively controlled. The formation mechanisms of the PPy/PET composite fibers and their corresponding carbon tubes have been studied with the aid of various spectroscopic and analytical methods. The investigations indicated that the morphological quality, integrity, and thickness of the PPy coating layer are the most crucial properties in determining the success of obtaining hollow and opened carbon tube structures. Observations with SEM on the pyrolyzed samples indicated that the PET core of a composite fiber started to melt between 230 and 290 °C and then decomposed and almost disappeared at ca. 390 °C, leaving behind only the hollow sheath. Both the diameter and wall thickness of such hollow tube further decreased as the treatment temperature elevated during the subsequent carbonization stage. The released gaseous, as well as the sublimed solid, byproducts during the carbon tube formation process were also monitored and investigated. All results of the present study indicate that PPy is thermally more stable than PET, thus suggesting that the carbon tube walls were mainly derived from the PPy skin layers.

Introduction

Studies on the formation and growth mechanism[1] of nanosized carbon tubes have attracted a lot of research interests in recent years, due to the interesting properties arising from their dimensions being comparable to molecular size and their potential in applications such as electron field emitters,[2] nanowires,[3] nanometer-sized probes,[4] natural gas storage, possible catalytic microreactors, and biosensors.[5] Various methods have been reported for the preparation of carbon tubes; these include carbon-arc discharge,[6] laser ablation,[7] condensed-phase electrolysis,[8] and the catalytic pyrolysis of hydrocarbons on various substrates such as porous anodic aluminum oxide,[9] fine metal particles,[10] and patterned cobalt layers.[11] Furthermore, it has also been demonstrated that various metal oxides[12] and some molecules such as small proteins[13] can be introduced into the cavity of nanotubes, followed by different reactions. Recently, we have also developed a novel method[14] for making carbon tubes by thermal pyrolysis of composite fibers that contained a thermally removable polymer core, like poly(ethylene terephthalate) (PET), and a thermally more stable skin, such as one made from a conducting polymer like polypyrrole (PPy). The present method can be used to prepare micrometer- or submicrometer-sized carbon tubes a few centimeters in length with a controllable tube wall thickness ranging from less than 30 nm to a few micrometers, by varying the thickness of the PPy skin layer. Furthermore, the tube diameter can also be varied by changing the diameter of the PET core fiber. Most interestingly, this new method enables the preparation of well-organized two-

* Corresponding author. E-mail: cchan@mx.nthu.edu.tw. Tel: 886-3-5724998. Fax: 886-3-5711082.

† Present address: Department of Pharmacy, Chia-Nan University of Science and Pharmacy, Tainan, Taiwan.

(1) (a) Iijima, S.; Ichihashi, T.; Ando, Y. *Nature* **1992**, *356*, 776. (b) Amelinckx, S.; Zhang, X. B.; Bernaerts, D.; Zhang, X. F.; Ivanov, V.; Nagy, J. B. *Science* **1994**, *265*, 635.

(2) (a) Heer, W. A. d.; Chatelain, A.; Ugarte, D. *Science* **1995**, *270*, 1179. (b) Heer, W. A. d.; Bonard, J.-M.; Fauth, K.; Chatelain, A.; Forro, L.; Ugarte, D. *Adv. Mater.* **1997**, *9*, 87.

(3) Ebbesen, T. W.; Lezec, H. J.; Hiura, H.; Bennett, J. W.; Ghaemi, H. F.; Thio, T. *Nature* **1996**, *382*, 54.

(4) (a) Dai, H.; Hafner, J. H.; Rinzler, A. G.; Colbert, D. T.; Smalley, R. E. *Nature* **1996**, 384, 147. (b) Wong, S. S.; Joselevich, E.; Woolley, A. T.; Cheung, C. L.; Lieber, C. M. *Nature* **1998**, *394*, 52.

(5) Freemantle, M. *Chem. Eng. News* **1996**, July 15, 62.

(6) (a) Iijima, S. *Nature* **1991**, *354*, 56. (b) Ebbesen T. W., Ajayan, P. M. *Nature* **1992**, *358*, 220.

(7) Thess, A.; Lee, R.; Nikolaev, P.; Dai, H.; Petit, P.; Robert, J.; Xu, C.; Lee, Y. H.; Kim, S. G.; Rinzler, A. G.; Colbert, D. T.; Scuseria, G. E.; Tomanek, D.; Fischer, J. E.; Smalley, R. E. *Science* **1996**, *273*, 483.

(8) Hsu, W. K.; Hare, J. P.; Terrones, M.; Kroto, H. W., Walton, D. R. M.; Harris, P. J. F. *Nature* **1995**, *377*, 687.

(9) Kyotani, T.; Tsai, L. F.; Tomita, A. *Chem. Mater.* **1995**, *7*, 1427.

(10) Endo, M. *Chemtech* **1988**, 568.

(11) Terrones, M.; Grobert, N.; Olivares, J.; Zhang, J. P.; Terrones, H.; Kordatos, K.; Hsu, W. K.; Hare, J. P.; Townsend, P. D.; Prassides, K.; Cheetham, A. K.; Kroto, H. W.; Walton, D. R. M. *Nature* **1997**, *388*, 52.

(12) (a) Ajayan, P. M.; Ebbesen, T. W.; Ichihashi, T.; Iijima, S.; Tangigaki, K.; Hirua, H. *Nature* **1993**, *362*, 522. (b) Ajayan, P. M.; Iijima, S. *Nature* **1993**, *361*, 333. (c) Tsang, S. C.; Chen, Y. K.; Harris, P. J. F.; Green, M. L. H. *Nature* **1994**, *372*, 159. (d) Lago, R. M.; Tsang, S. C.; Chen, Y. K.; Green, M. L. H. *Chem. Commun.* **1995**, 1355. (e) Kuan, Y.; Green, M. L. H.; Tsang, S. C. *Chem. Commun.* **1996**, 2489.

(13) Tsang, S. C.; Davis, J. J.; Green, M. L. H.; Hill, H. A. O.; Leung, Y. C.; Sadler, P. J. *Chem. Commun.* **1995**, 1803.

(14) Han, C. C.; Lee, J. T.; Yang, R. W.; Chung, H.; Han, C. H. *Chem. Commun.* **1998**, 2087.

10.1021/cm010141f CCC: $20.00
Published on Web 07/11/2001

or three-dimensional structures assembled by carbon tubes several centimeters in length via the use of appropriate woven templates,[15] which should enable easier design and fabrication of actual articles for various practical applications.

The present paper is directed at understanding the formation mechanism of these novel carbon tubes with the aids of various spectroscopic and analytical methods. The change in morphology and shape of the PPy/PET composite fibers after being subjected to a single heat treatment at various temperatures, ranging from RT (room temperature) to 1000 °C, was observed with scanning electron microscopy (SEM). Moreover, the thermal degradation chemistry of these composite fibers was studied with thermogravimetric analysis (TG), differential scanning calorimetry (DSC), and elemental analysis (EA). The evolved gas from thermal degradation was monitored with pyrolysis IR and also with thermogravimetric analysis coupled with mass spectrometry (TG-MS). The sublimed solids obtained during the thermal decomposition process were collected and studied with NMR, IR, and mass spectroscopies. The formation mechanism of carbon tubes is thus clearly established. Furthermore, the crucial roles played by the morphology and the growth mechanism of the PPy skin layer in determining its tube-forming ability have also been addressed.

Although the current study is focused on the micrometer-sized carbon tubes as prepared from micrometer-sized PPy/PET composite fibers that utilized commercially available micrometer-sized and submicrometer-sized PET as the core fibers, it is envisaged that such preparation method and chemical insights for carbon-tube formation will also be applicable for future preparation of nanometer-sized carbon tubes using the recently developed nanometer-sized fibers[16] as the core fibers.

Experimental Section

Materials. The poly(ethylene terephthalate), PET, fibers (16.7, 7.5, 2.5, and 0.8 μm in diameter) were obtained from Far Eastern Textile Co. Ltd. (Hsinchu County, Taiwan) and Union Chemical Laboratories, Industrial Technology Research Institute (Hsinchu, Taiwan). Pyrrole was obtained from Aldrich and distilled under vacuum to remove brown aged products before use. *p*-Toluenesulfonic acid monohydrate (Aldrich, 98%) and ammonium persulfate (Aldrich, 98%) were used without further purification. The resistance of the deionized water used for experiments was 18.2−18.3 MΩ. The polypyrrole (PPy) coated PET composite fibers were prepared via a typical reaction-coating approach[17] using the previously reported procedure,[15] by first suspending commercially available PET fibers (1 g) in a 0.02 M pyrrole aqueous solution (120 mL) containing a 2 equiv amount of *p*-toluenesulfonic acid, followed by the addition of 0.025 M APS aqueous solution (120 mL). A reaction coating time of 30 min was used. The thickness of such PPy coating layers can be controlled by increasing the number of reaction coating treatment cycles. The PPy control sample was prepared similarly, except by using 20-fold more concentrated solutions of corresponding reagents in the absence of the PET fibers. The carbon tubes were prepared by heating the above PPy/PET composite fibers in a quartz tube oven from room temperature to 1000 °C at a heating rate of 10 °C/min under N_2 atmosphere (N_2 flow rate 0.5 L/min). An annealing time of 0−3 h was employed after the temperature reached 1000 °C, before the carbon tubes were cooled to ambient temperature.

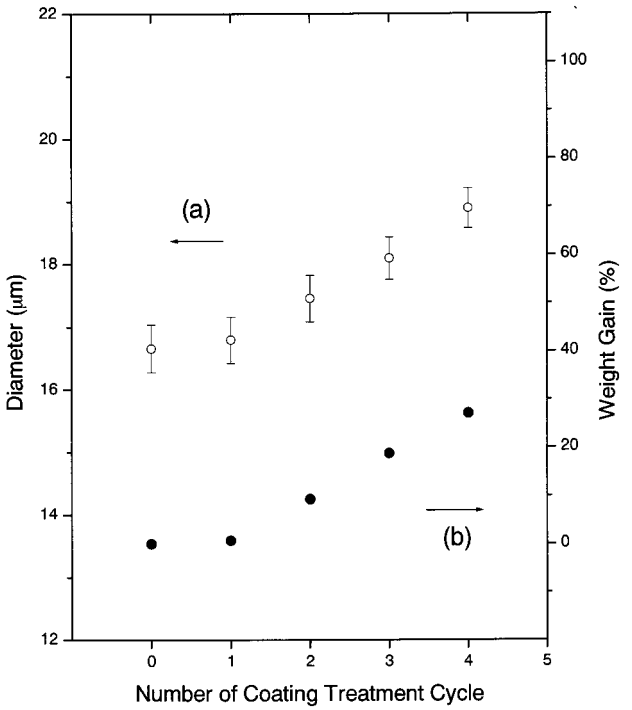

Figure 1. Diameter (open circle) and percentage weight gain (solid circle) of the PET core fiber and PPy/PET composite fibers after 1−4 cycles of reaction coating treatment.

The morphology and shape of the various samples were observed by scanning electron microscopy (SEM) on a Hitachi S-2300 microscope or by field emission scanning electron microscopy (FESEM) using Hitachi S-4000 equipment, both using an accelerating voltage of 20 kV. The surface of samples was typically coated with a thin film of Pt/Pd (4/1) or Au (ca. 50−200 Å thick) before SEM studies, for charge dissipation purpose. Differential scanning calorimetry (DSC) experiments were performed on Seiko Instruments model SSC5200 analyzer, from −100 to 350 °C at a heating rate of 5 °C/min using a nitrogen flow rate of 40 mL/min. Thermogravimetric analysis in conjunction with differential thermal analysis (TG-DTA) was performed with a Seiko Instruments model SSC5200 analyzer. Samples for TG studies were heated from 30 to 1000 °C with a heating rate of 10 °C/min using nitrogen, at a flow rate of 100 mL/min. The evolved gaseous byproducts resulting from the thermal degradation of composite fiber, PET fiber, and the PPy control sample were also investigated with pyrolysis IR and thermogravimetric analysis coupled with mass spectrometry (TG-MS) using a thermogravimetric analyzer (Seiko SSC5000 Analyzer) coupled to a VG mass spectrometer. The range of *m*/*z* ratios selected for mass spectroscopy analysis was from 5 to 303. The transfer line between TG and MS instruments was kept warm at ca. 200 °C, and the carrier gas (He) was maintained at a flow rate of 100 mL/min. Elemental analysis (EA) was performed using a Heraeus CHN-Rapid Elemental Analyzer. The nitrogen, carbon, and hydrogen contents were measured.

Results and Discussion

Formation of PPy/PET Composite Fibers. The diameters of the PPy-coated PET fibers composite fibers prepared by the reaction-coating approach[15,17] are summarized in Figure 1 and were found to be directly

(15) Han, C. C.; Lee, J. T.; Yang, R. W.; Chung, H.; Han, C. H. *Chem. Mater.* **1999**, *11*, 1806.
(16) Kageyama, K.; Tamazawa, J.-I.; Aida, T. *Science* **1999**, *285*, 2113.
(17) Gregory, R. V.; Kimbrell, W. C.; Kuhn, H. H. *Synth. Met.* **1989**, *28*, C823.

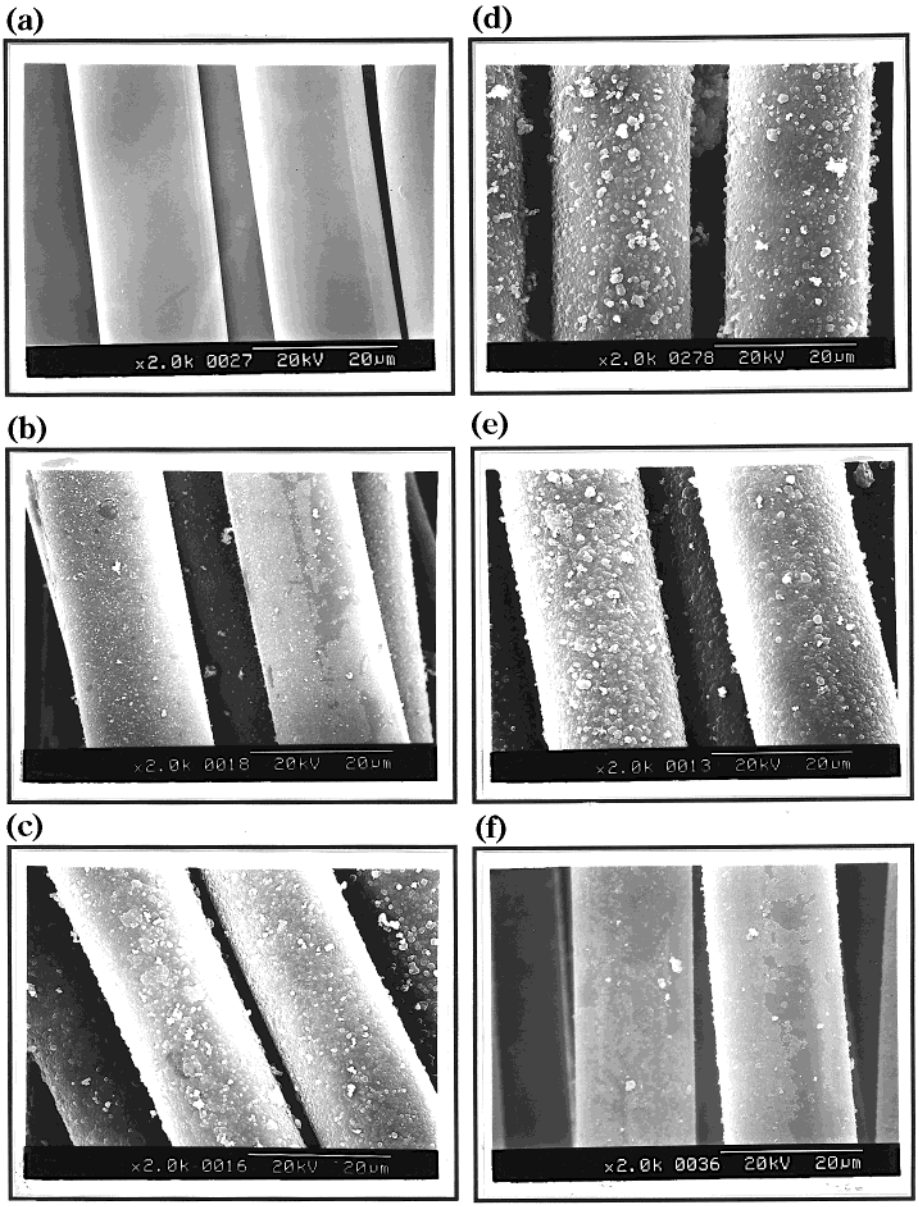

Figure 2. SEM micrographs (all with a magnification of 2000 times) for (a) uncoated PET fibers (averaged diameter ca. 16.7 μm), (b−e) PET fibers after being treated with PPy reaction coating for 1, 2, 3, and 4 cycles, respectively, and (f) PET fibers after 1 cycle of PPy coating but treated with 4-fold the amounts of pyrrole and oxidant, using a quadruple reaction period.

proportional to the number of coating treatments, viz. 16.8(±0.4), 17.5(±0.4), 18.1(±0.3), and 18.9(±0.3) μm, after the PET fiber (ca. 16.7 ± 0.4 μm) went through one, two, three, and four cycles of PPy coating treatment, respectively, while the corresponding % weight gain of the respective fiber (Figure 1), based on the weight of the original uncoated PET fiber, was 0.66%, 9.3%, 18.7%, and 27.1%.

Interestingly, under the same coating treatment conditions and duration, both the increase in diameter and the weight gain of the PPy/PET composite fiber from the first coating cycle were much less than that obtained from each of the subsequent coating cycles. The results indicated that the growth of PPy skin layer on the PET surface in the first coating cycle was significantly slower than subsequent coating cycles, with each subsequent cycle obtaining a similar weight of PPy. After the initial reaction coating treatment, the original white and smooth surface of the PET fibers (Figure 2a) turned black and was covered with PPy depositions having a nodular morphology (Figure 2b−e). The SEM micrographs in Figure 2 indicated that the PPy coating layers resulting from multiple coating cycles were rather thick (from ca. 0.40 to ca. 1.12 μm) and homogeneous in feature, whereas the PPy layer from the first coating cycle was much thinner (ca. < 0.07 μm) and incomplete, with some of the original PET fiber surface still exposed (Figure 2b). Judging from the shape and distribution of the exposed areas, we believe they were caused by dislodging/peeling of the loosely bonded PPy coating when the fiber was stripped or rubbed during the washing and sample handling operations. The differences in morphology and thickness (and weight gain) between the PPy layers from the first and subsequent coating cycles imply that different formation mechanisms for the corresponding PPy skin layers may be involved.

Further investigations with SEM microscopy (Figure 3) clearly showed that the diameter of the resulted nodules on the PPy layer actually increased with the

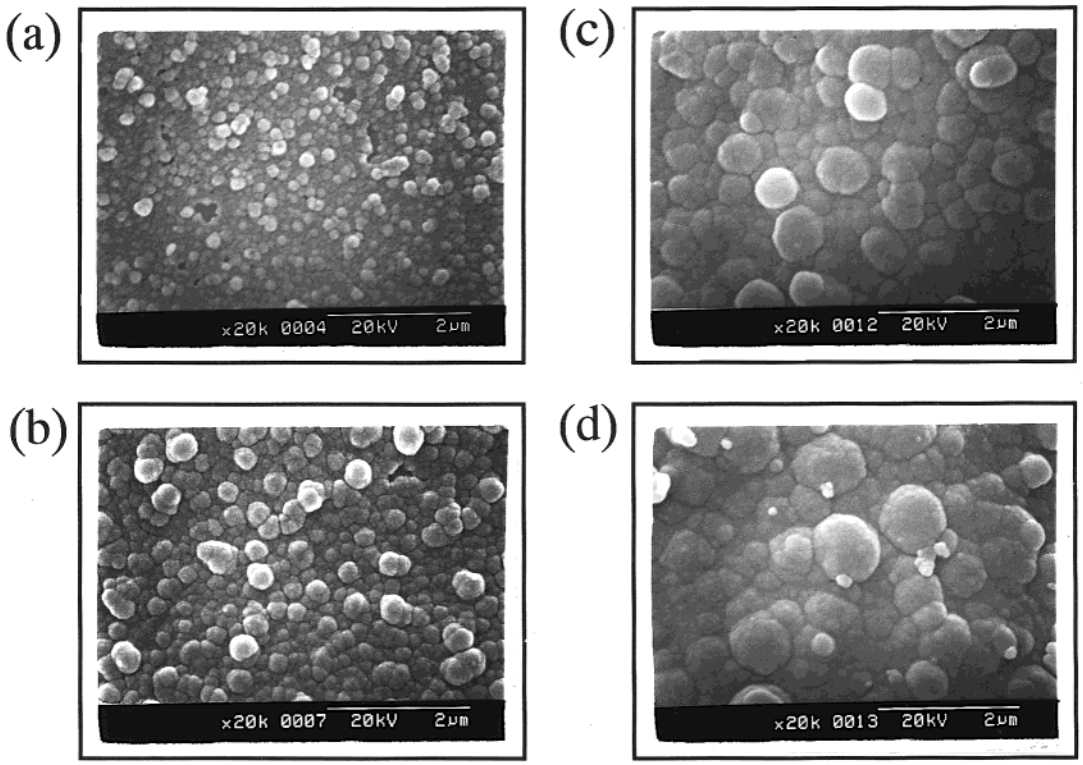

Figure 3. SEM micrographs for the PPy layers (all with a magnification of 20 000 times) of the PPy/PET composite fibers: (a−d) 1, 2, 3, and 4 coating treatment cycles, respectively.

number of coating cycles; the average diameter of the nodules was measured to be 91(±40), 260(±90), 420-(±180), and 510(±210) nm after one, two, three, and four coating cycles, respectively. To further explore the possible growing mechanisms for the PPy layers, a control experiment was conducted by performing a single coating cycle using the same amount of PET fibers but with 4-fold amounts of both pyrrole and oxidant (equivalent to the accumulated amounts of both reagents used for preparing a four-cycle coated composite fiber) and quadruple the coating reaction time (i.e. 120 min instead of 30 min). Surprisingly, the resulted composite fiber (Figure 2f) was still only coated with a rather thin PPy layer, with a weight gain of only 0.66 wt %, comparable to the 0.69 wt % for a normal one-cycle-coated sample. Moreover, the size of the PPy nodules on the PET fiber surface resulted from this control experiment was found to be ca. 104(±34) nm, again comparable to the 91(±40) nm for the normal one-cycle-coated sample. Furthermore, for all first coating cycles, a large amount of free PPy particles always formed in the solution phase, whereas hardly any PPy particles were found in the solutions phases for all subsequent coating cycles.

On the basis of the above results, a plausible PPy skin layer formation mechanism is suggested for different coating cycles. It is believed that most of the PPy particles in the first coating cycle might have initiated and continued their growth in the solution phase, and only those particles (or the growing PPy chains) at or close to the liquid/solid interfaces had deposited onto the PET fibers via chemisorption and/or physical adsorption. Since the growth of PPy on the fiber surface has to compete with the more numerous PPy growing centers in solution, for the limited amount of pyrrole, it is not surprising that the resulting PPy layer is thinner than the PPy layers from subsequent coating cycles, of which most of the PPy coatings might have been grown directly on the surface of the existing PPy layer, due to the lower oxidation potential of the PPy surface. Typically, the oxidation potential of the PPy is in the range of −0.05 to 0.15 V (vs Ag/AgCl),[18a] which is much lower than the 1.2 V for pyrrole monomers.[18b] Such great difference in oxidation potentials makes the polymerization of pyrrole (via an oxidative coupling pathway[19]) for subsequent coating cycles initiated predominantly and propagated preferentially at the surface of the already deposited PPy layer. Such utilization of PPy surface in subsequent coating cycles as the polymerization center would first increase the size of the PPy powders/nodules at the surface and eventually result in a highly intercalated networklike PPy coating layer, which is also like a sheath over the PET core fiber. This proposed coating mechanism can account for the continuous size-increase phenomena for the surface PPy nodules with the number of coating cycles and for the much better adhesion between the PPy layers (and/or PPy nodules) from different coating cycles, as evidenced by the absence of dislodge features on the surfaces of the composite fibers after the first coating cycle.

Furthermore, the apparent density of these PPy skin layers on the PET fibers was calculated using the weights and volumes of the corresponding PPy layers, yielded from the third or the fourth treatment cycles, to have an average value of 1.23 g/cm^3. Such density

(18) (a) Qiu, Y.-J.; Reynolds, J. R. *Polym. Eng. Sci.* **1991**, *31*, 417. (b) Diaz, A. F.; Bargon, J. In *Handbook of Conducting Polymers*; Skotheim T. A., Ed.; Marcel Dekker: New York and Basel, 1986; Vol. 1, Chapter 3.

(19) (a) *Handbook of Organic Conductive Molecules and Polymers*; Nalwa, H. S., Ed.; John Wiley & Sons: Chichester and New York, 1997; Vols. 1−4. (b) *Handbook of Conducting Polymers*; Skotheim, T. A., Ed.; Marcel Dekker: New York and Basel, 1986; Vols. 1−2.

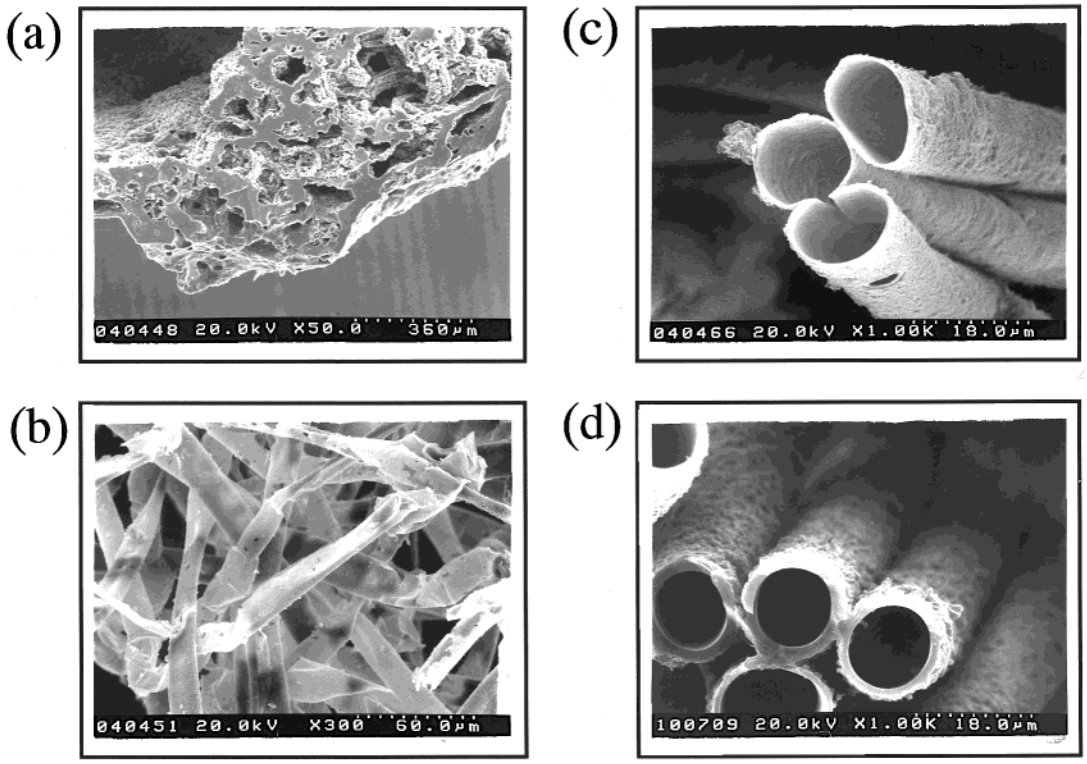

Figure 4. SEM micrographs for the thermally treated samples, at 1000 °C for 3 h under a N_2 flow at 0.5 L/min, prepared from the PPy/PET composite fibers that have been treated with (a) one, (b) two, (c) three, and (d) four cycles of PPy coating.

value is very comparable to the previously reported apparent density (1.24 g/cm^3) for a typical PPy film doped with *p*-toluenesulfonic acid.[20] This result suggests that the PPy skin layers obtained from the multiple coating cycles may have a structure similar to that of a typical free-standing PPy film.

Controls on Diameter and Wall Thickness of Carbon Tubes. The diameter and wall thickness of final carbon tubes can be conveniently controlled by varying the diameter of the corresponding core fiber and the thickness of the polypyrrole coating layer.[15] In general, the wall thickness and the diameter of the resultant carbon tubes are directly proportional to the thickness of the PPy coating layer and the diameter of the PET core fiber, respectively. Furthermore, it is noteworthy that the composite fibers from the first coating cycle turned into a mass of fused porous carbon matrix, instead of forming carbon tubes or retaining their filamentous structure (Figure 4a). This result may be attributed to the fact that the PPy skin layer of these composite fibers (Figure 2b) was too thin and too weak to survive the expansion and hollowing of the PET core when the core was heated under increasing temperature. Thus, such result also confirmed that the walls of carbon tubes were mainly converted from the PPy skin layers and suggested that the morphological quality and integrity of the PPy layer were the most crucial parameters for successful carbon tube formation. The SEM micrograph in Figure 4b shows however that although carbon tubes can be made from the composite fibers obtained after two coating cycles, all tubes were collapsed. This may be ascribed to insufficient tube wall mechanical strength, due to their small thickness of only ca. 0.37($\pm$0.10) μm, to retain structural integrity during the tube formation process, or to support the hollow circular-tube structure with this relative large diameter (ca. 16 μm). Similar collapsed tube structures had also been observed and reported in some works related to nano carbon tubes.[21] On the other hand, if the tube wall was thick enough, like those carbon tubes (Figure 4c,d) produced from the composite fibers after the third and fourth coating cycles, intact open-tube structures can be easily obtained. Interestingly, the minimum wall thickness required for supporting an open-tube structure was actually dependent on the diameter of the carbon tubes. In general, as the diameter of the carbon tubes became smaller, such minimum wall thickness also decreased. For instance the minimum wall thickness of carbon tubes having diameters of about 16, 7, 1.8, and 0.73 μm was about 500, 250, 70, and 30 nm, respectively. Such a relationship is consistent with the fact that, for a given tube wall thickness, a smaller curvature (i.e. tube diameter) will give rise to stronger structure. The same results may also account for the ability of nano carbon tubes in maintaining their round-shaped open-tube structures, despite their relative thin tube walls. Figure 5 depicts the relationship between the minimum wall thickness required for maintaining an open-tube structure for a given diameter of carbon tube; the straight line is constructed by least-squares fitting while forcing it to go through the origin. On the basis of the slope of the straight line, it can be estimated that a tube wall thickness of ca. 0.2$-$0.3 nm (i.e., 1 atom thick layer) will be strong enough to support an open tube with a diameter of ca. 1$-$10 nm. Although the exact relationship between the required minimum wall thick-

(20) Qian, R.; Qin, J. *Polym. J.* **1987**, *19*, 157.

(21) Endo, M.; Takeuchi, K.; Igarashi, S.; Kobori, K.; Shiraishi, M.; Kroto, H. W. *J. Phys. Chem. Solids* **1993**, *54*, 1841.

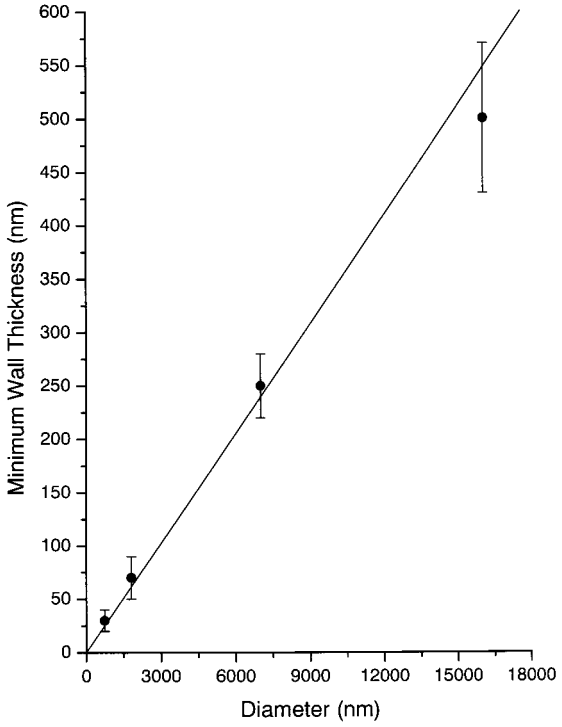

Figure 5. Minimum wall thickness required for maintaining an open-tube structure as a function of the diameter of corresponding carbon tubes. The linear fit had been forced through the zero point.

ness and open-tube diameter still needs to be further clarified and the mechanical strength characteristic might vary widely between different carbon phases (e.g. amorphous vs graphitic), the above crude analysis seemed to agree with the general trend that have been observed so far for multiwalled,[1] as well as single-walled, nano carbon tubes.[7,22]

Formation of Carbon Tubes. The formation mechanism of carbon tubes was further investigated with SEM using the PPy/PET composite fibers that were prepared from the 16.7 μm PET fibers with four cycles of PPy coating treatments. These composite fibers were heated from 30 °C to a given temperature between 30 and 1000 °C (at 10 °C/min) in a quartz tube oven under a N_2 flow (at a rate of 0.5 L/min) and cooled naturally to room temperature when the given temperature was reached. The morphology and appearance of these thermally treated samples were observed with SEM. The SEM micrographs for the samples being heated at 230, 290, 340, 390, 680, and 1000 °C were selected and displayed in Figure 6a−f. The SEM micrograph in Figure 6a (for the 230 °C sample) indicated that no significant change in appearance was found for the composite fiber if the sample was heated below the melting point, i.e., 254 °C, of the PET core fiber. [The melting point of the PET core fibers, as measured by DSC (differential scanning calorimetry), was 254 °C, and their initial and onset decomposition temperatures, as measured by TG, were ca. 358 and 407 °C, respectively.] When the treatment temperature was higher than 254 °C, the PET core of the composite fiber started to melt, as illustrated by the SEM micrograph in Figure 6b for the 290 °C sample. At higher temperatures, such as 340 °C, some molten materials had even flowed out of the tube and appeared on the outside surface of the PPy skin layers, as showed by the micrograph in Figure 6c. At this point, some of the PPy/PET composite fibers started to form a hollow tube structure with the PPy skin layers remaining unchanged and retaining their round shapes. When the sample was heated to a temperature, e.g. 390 °C, which is slightly above the initial thermal decomposition temperature for PET fiber (i.e. 358 °C), most of the core PET and the molten PET on the PPy surface were decomposed and disappeared, leaving behind the round-shaped hollow tubes with rather clean surfaces (Figure 6d).

As the treatment temperatures went higher than 390 °C, the shape and morphology of these hollow tubes remained similar; however, both the tube diameter and wall thickness gradually decreased with increased treatment temperature. For example, the wall thickness was found to decrease from 2.3(±0.3) to 1.4(±0.3) μm, when the treatment temperature was increased from 390 to 1000 °C; meanwhile the outer diameter of the same sample decreased from 18.3(±0.4) to 16.7(±0.6) μm, and the inner diameter from 13.7(±0.6) to 13.5-(±0.7) μm. Such decrease in tube diameter or wall thickness with heating temperature can be noticed by the SEM micrographs, as displayed in Figure 6d−f, for samples being treated at 390, 680, and 1000 °C, respectively. Detailed information about changes in tube wall thickness and diameters vs annealing temperature is summarized in Table 1. The reduction in outer diameter is consistent with the previously reported dimensional contraction of ca. 20% for the three-dimensional carbon tube assembly, similarly prepared from PPy-coated PET cloth.[15] Such contraction may be caused by the formation of a more densely packed and highly networked structure within each PPy skin layer, as the annealing temperature was elevated, similar to the networking transformation associated with the elimination of HCN or N_2 during the carbonization of polyacrylonitrile.[23]

The weight retention (%) of the samples after the thermal treatment under N_2 flow in an quartz tube oven, also summarized in Table 1, shows a similar trend as that obtained by TG analysis for the PET fiber.[15] However, there is a general shift toward lower temperatures for the composite fiber sample. This may be at least partly attributed to the acid-catalyzed decomposition effect[24] of PET, due to the presence of residual acid dopant, TsOH, in the PPy skin layer. Furthermore, the same results also indicated that the rate of weight loss became much lower, at temperatures above 390 °C, after the formation of hollow tubes. Such weight reduction was accompanied by the above-mentioned decrease in diameters and wall thickness, together with the decrease in N/C atomic ratio measured by elemental analysis (as discussed in the following section). Obviously, the degradation that happened at above 390 °C

(22) (a) Iijima, S.; Ichihashi, T. *Nature* **1993**, *363*, 603. (b) Bethune, D. S.; Kiang, C. H.; de Vries, M. S.; Gorman, G.; Savoy, R.; Vazquez, J.; Beyers, R. *Nature* **1993**, *363*, 605.

(23) (a) Savage, G. *Carbon-Carbon Composites*; Chapman & Hall: London, 1993; p 48. (b) Henrici-Olivé, G.; Olivé, S. In *Industrial Developments* (*Advances in Polymer Science, 51*); Springer-Verlag: Heidelberg, Germany, 1983; p 1.

(24) Montaubo, G.; Puglisi, C.; Samperi, F. *Polym. Degrad. Stab.* **1993**, *42*, 13.

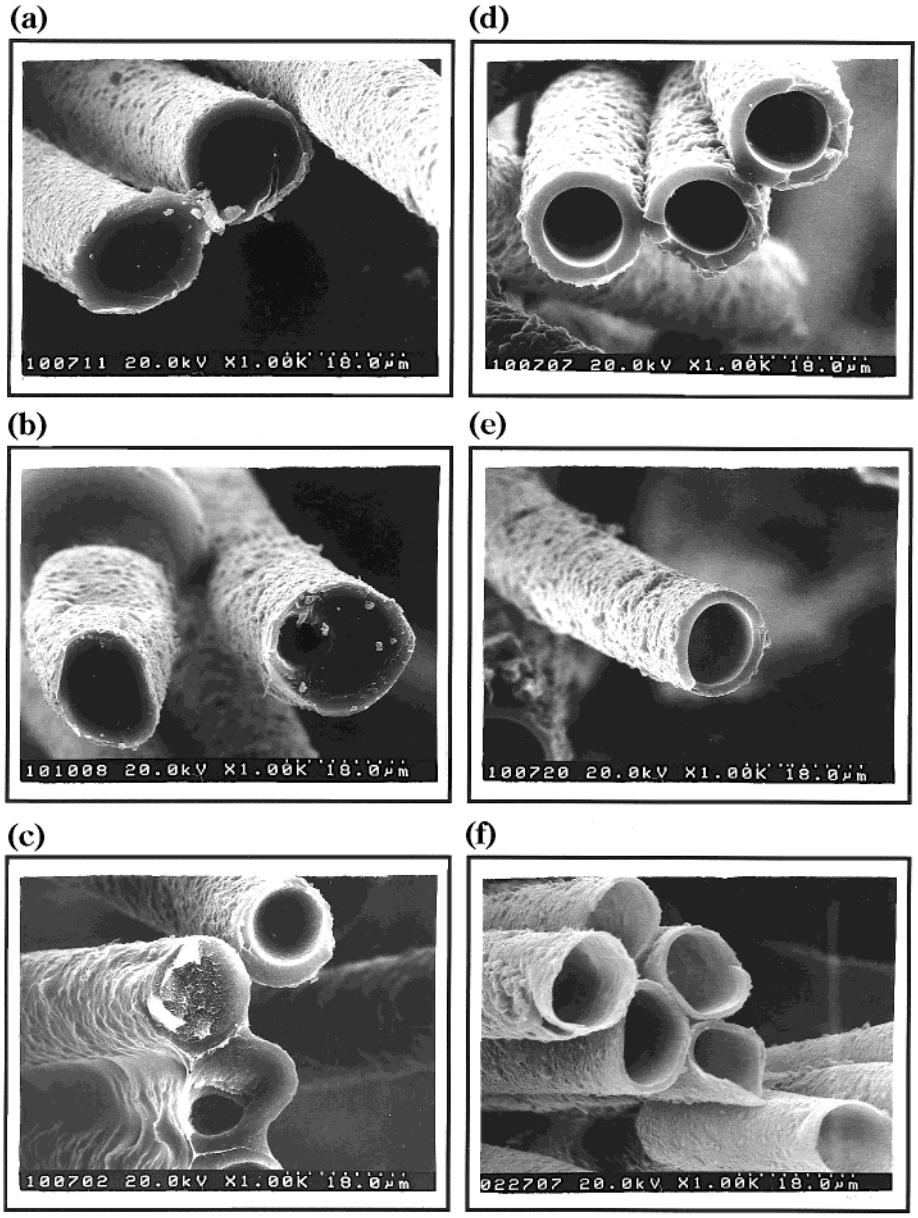

Figure 6. SEM micrographs for the PPy/PET composite fibers, having four cycles of PPy coating treatment, after being thermally treated at (a) 230 °C, (b) 290 °C, (c) 340 °C, (d) 390 °C, (e) 680 °C, and (f) 1000 °C.

Table 1. Change of Tube Diameter, Wall Thickness, and Weight Retention for Thermally Annealed Samples of PPy/PET Composite Fibers

annealing temp (°C)	outer diameter (μm)	inner diameter (μm)	wall thickness (μm)	weight retention (%)
RT	18.9(±0.3)			100
190				96
230				94
290				92
340				77
390	18.3(±0.4)	13.7(±0.6)	2.3(±0.3)	34
440	18.1(±0.6)	13.6(±0.6)	2.2(±0.3)	31
560	18.0(±0.5)	13.3(±0.6)	1.9(±0.3)	30
680	17.0(±0.5)	13.0(±0.7)	1.7(±0.3)	29
830	16.8(±0.3)	12.9(±0.7)	1.6(±0.3)	28
1000	16.7(±0.6)	13.5(±0.7)	1.4(±0.3)	26

was a typical carbonization process and had clearly involved the N-containing PPy layer, thus accounting for the liberation of various N-containing byproducts. The more detailed degradation information and chemistry will be presented and discussed in the following section.

Evolved Gaseous Byproducts from Thermal Degradation. For a better understanding on the thermal degradation mechanism, the gaseous byproducts evolved during the thermal treatment of the composite fibers were collected from RT to 1000 °C, at every 50 °C interval, and were then analyzed by FTIR (Perkin-Elmer 2000) at a spectral resolution of 0.5 cm^{-1} using a gas cell equipped with a pair of NaCl windows. Most of the gaseous byproducts were found to evolve between 200 and 800 °C, and they were identified to be CO, CO_2, CH_3CHO, methane, ethene, H_2O, acetylene, SO_2, and HCN. The IR spectra for the gas samples collected at different temperature ranges, such as 50−100, 300−350, 400−450, and 650−700 °C, are displayed in Figure 7a−d.

For a better understanding on the origin of each gaseous degradation byproduct, two control experiments were performed, using the same methods and conditions to thermally degrade the individual component of the composite fiber, i.e., the PET core fiber and a control

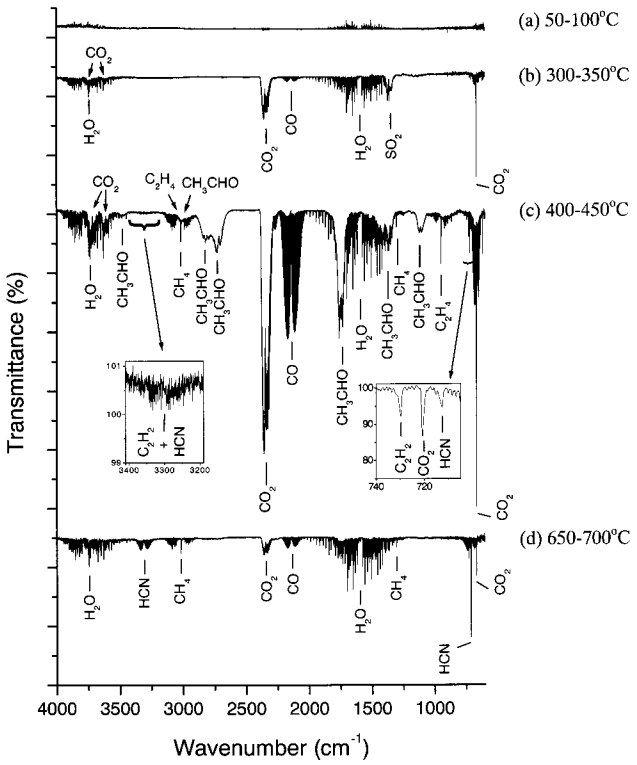

Figure 7. Infrared spectra for the gaseous byproducts evolved in the temperature range of (a) 50−100 °C, (b) 300−350 °C, (c) 400−450 °C, and (d) 650−700 °C. (Spectral resolution was 0.5 cm^{-1}.)

sample of PPy powder. Judging from the above results and the outcomes from control experiments, we believed that the byproducts such as CO, CO_2, CH_3CHO, ethene, acetylene, and H_2O came mainly from the thermal decomposition of the PET core fiber. Similar gaseous byproducts from the thermal degradation of PET had also been observed before,[29] whereas the gaseous byproducts, such as CH_4 and HCN, resulted from the decomposition of the PPy skin layer. Furthermore, the gaseous products from the PET core fiber were liberated at a relatively lower temperature range (i.e. <500 °C) than those from the PPy skin layer (i.e. >500 °C). This finding is consistent with the observation that PPy was thermally more stable than PET.[15] Interestingly, some SO_2 gas was also unexpectedly present when heating the composite fiber at between 200 and 500 °C. After comparison with the results from the above control experiments, the SO_2 was proved to originate from the PPy skin layer. We believe that SO_2 was probably resulted from the decomposition of the residual dopant, TsOH, within the PPy matrix. This result is consistent with the general observation that conducting polymers are very difficult to be dedoped completely and that thermal elimination of the TsOH dopant from conducting polymer matrixes generally started at ca. 240 °C.[19]

Interestingly, although a small amount of NH_3 gaseous byproduct was detected between 500 and 1000 °C (with a maximum output at 600−650 °C) in the control experiment, using a control sample of PPy powder, it was however not observed when the PPy/PET composite fibers were heated. This result may be attributed to the trapping of the NH_3 gas by the sublimed acidic solid byproducts (as discussed in the following section), such as terephthalic acid from the PET core.

The evolutions of the gaseous byproducts were also investigated with TG-MS, using the composite fibers, the PET core fibers, and the control sample of PPy powder. The representative results are summarized and displayed in Figure 8. The results showed that the gaseous byproducts originated from the PET fiber, such as CO (m/z = 28*, 16, 12 at 418 °C), CO_2 (m/z = 44*, 28, 16, 12 at 418 °C), ethene (m/z = 28*, 27, 26 at 418 °C), ethanal (m/z = 44, 43, 29*, 27 at 418 °C), and acetylene (m/z = 26*, 25 at 413 °C), were all liberated below 500 °C. [The selected m/z values are displayed in parentheses with the base peak being marked with an asterisk.] Whereas the gaseous byproducts originated from the PPy coating, such as HCN (m/z = 27*, 26 at 637 °C), were mainly given off at above 500 °C. In addition, the N_2 (m/z = 28*, 14) byproduct, which was found to evolve from ca. 600 to 1000 °C, although being IR-inactive, could be easily observed by TG-MS study. Similar denitrogenation phenomenon had also been observed during the carbonization of polyacrylonitriles in the same temperature range.[30] The above results are consistent with the fact that PPy skin layer is thermally more stable than the PET core fiber.

Furthermore, the above TG-MS results also confirmed that the evolution of SO_2 (m/z = 64*, 48, 32, 16) at 248 and 422 °C was all originated from the PPy skin layer. After comparing with the results from other control experiments, using doped and undoped control samples of PPy powder, we believe that both SO_2 peaks were all associated with the residual TsOH dopant within the matrix of the PPy skin layer. Interestingly, the results also indicated that only the SO_2 evolution peak at 422 °C occurred concurrently with the evolution of the expected counter tolyl fragment (m/z = 92, 91*, 77). The results implied that these two SO_2 evolution peaks might be associated with two very different decomposition mechanisms that involved different TsOH dopant forms (such as the sulfonate or sulfonic acid forms). The evolution of SO_2 gas during the thermal degradation of TsOH-doped PPy had also been previously observed in a preliminary and brief study using Fourier transform infrared/evolved gas analysis (FTIR/EGA).[31] Although the same report did not mention or discuss any other possible byproducts (such as HCN, N_2, and the tolyl fragment), the result however did display a similar twin peak pattern for the evolved SO_2 gas. Currently efforts are being made to investigate the possible mechanistic cause for each SO_2 evolution peak.

Apparently, all the nitrogen-containing byproducts, such as HCN and N_2 (and also possibly including NH_3), were contributed from the decomposition of the PPy layer. The elimination of HCN occurred between 240

(25) Pouchert, C. J. *The Aldrich Library of FT-IR Spectra,* 1st ed.; Aldrich Chemical Co.: Milwaukee, WI, 1989; Vol. 3.
(26) (a) Frisch, M. J.; Schaefer, H. F., III; Binkley, J. S. *J. Phys. Chem.* **1985**, *89*, 2192. (b) Callomon, H. J.; Hirota, E.; Kuchitsu, K.; Lafferty, W. J.; Maki, A. G.; Potein, C. S. In *Numerical Data and Function Relationships in Science and Technology*; Hellwege, K. H., Ed.; Springer-Verlag: West Berlin, 1976; Vol. 7.
(27) Kim, K.; King, W. T. *J. Chem. Phys.* **1979**, *71*, 1967.
(28) Socrates, G. *Infrared Characteristic Group Frequencies. Tables and Charts*, 2nd ed.; John Wiley & Sons: New York, 1994.
(29) Buxbaum, L. H. *Angew. Chem., Int. Ed. Engl.* **1968**, *7*, 182.
(30) Watt, W. *Carbon* **1972**, *10*, 121.
(31) Trung, V. T.; Ennis, B. C.; Turner, T. G.; Jenden, C. M. *Polym. Int.* **1992**, *27*, 187.

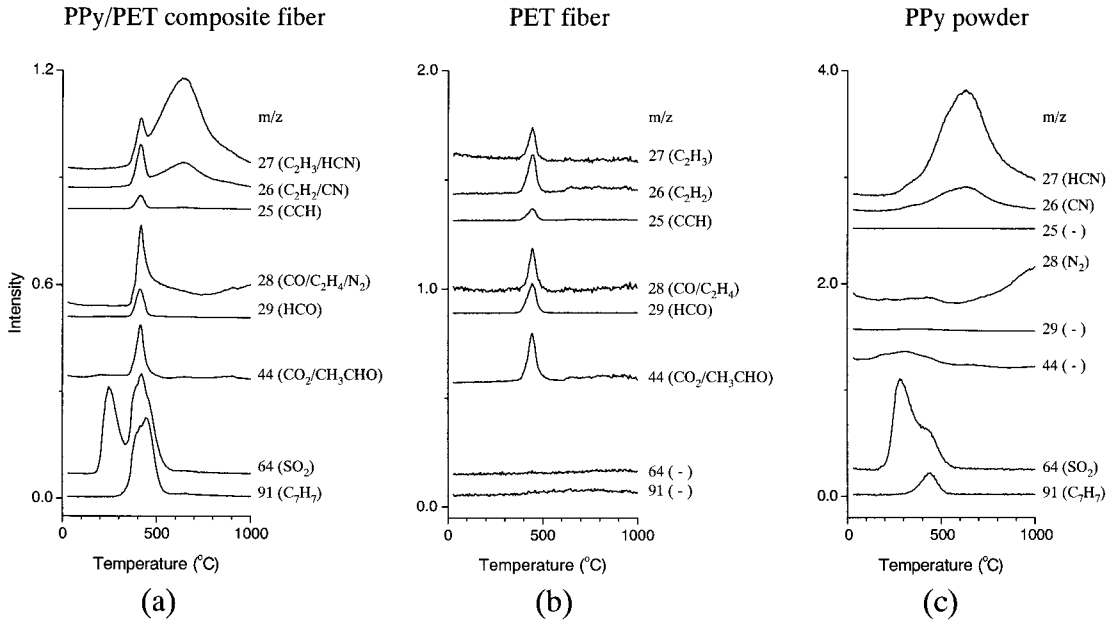

Figure 8. TG-mass spectra for (a) PET/PPy composite fibers, (b) PET core fibers, and (c) control samples of PPy powder. The absolute intensity scale for the peaks of *m/z* 28, 29, and 44 is used herewith. For viewing clarity, the intensities of *m/z* 25, 26, and 27 have been enlarged by a factor of 6.5 and those of *m/z* 64 and 91 by a factor of 27.

and 1000 °C and peaked at 637 °C; whereas the denitrogenation process started at much higher temperatures at above 600 °C. The elimination of nitrogen-containing byproducts should lead to a lowering of N content in heated composite fiber samples; such lowering had been confirmed by the reduction in the N/C atomic ratios as measured by elemental analysis (EA). The EA results indicated that the N reduction rate in the heated composite fibers peaked at ca. 638 °C. Such results coincided with the finding from TG-MS study for the heated composite fiber (Figure 8a), which showed an evolution peak for major N-containing byproducts, HCN, at ca. 637 °C. Interestingly, both IR and TG-MS studies did not observe any cleavage of pyrrole monomer (bp 131°C) or oligomers from the PPy backbone. The result again confirms the high thermal stability of PPy backbones and explains why PPy gave relative higher char yield than PET fiber.[15]

Sublimed Solids from Thermal Degradation. Besides the gaseous byproducts discussed above, some off-white to light yellow colored solid byproducts had also been found to condense on the wall of the quartz tube just outside the heating zone, at the downstream end of the nitrogen flow. It was observed that most of the solids were sublimed out of the oven between about 350 and 450 °C, consistent with the main decomposition temperature range of the PET core fibers. These sublimed solids were collected, separated by column chromatography, and characterized with IR and NMR. As reported previously,[15] the condensed solids mainly consisted of terephthalic acid and 4-(vinyloxycarbonyl)-benzoic acid. Apparently, they were produced from the thermal decomposition of the PET core fibers. Such chemical information was however complicated by the observation that the 4-(vinyloxycarbonyl)benzoic acid byproduct was very sensitive to the handling processes of separation and storage and can be easily converted to terephthalic acid by losing an acetylene moiety via either a β-hydrogen elimination or a 1,5-hydrogen shift rearrangement.[15] To minimize further decomposition of the sublimed degradation byproducts, i.e., 4-(vinyloxycarbonyl)benzoic acid, the composite fibers were heated, in another control experiment, from RT to ca. 600 °C instead of to 1000 °C. After separation and purification, a small amount of a new solid byproduct, i.e., bis-(vinyloxycarbonyl)benzene, was obtained in addition to the two original byproducts of terephthalic acid and vinyloxycarbonyl benzoic acid.[15] [Data for 1,4-bis(vinyloxycarbonyl)benzene: ^{1}H NMR (400 MHz, $CDCl_3$) δ 8.13 (s, 4H), 7.44 (dd, 1H, $J_{ab} = 13.8$ Hz, $J_{ac} = 6.1$ Hz), 5.06 (dd, 1H, $J_{ba} = 13.8$ Hz, $J_{bc} = 1.8$ Hz), 4.70 (dd, 1H, $J_{ca.} = 6.1$ Hz, $J_{cb} = 1.8$ Hz); ^{13}C NMR (100 MHz, $CDCl_3$) δ 162.72 (C), 141.27 (CH), 133.30 (C), 130.03 (CH), 98.94 (CH_2); IR (KBr pellet, cm^{-1}) 3119, 3102, 3061, 1731, 1654, 1409, 1306, 1258, 1237, 1145, 1094, 952, 890, 871, 847, 723, 691; mass *m/z* 218 (M^+), 175 ($M^+ - OC_2H_3$, 100), 147 ($M^+ - CO - OC_2H_3$), 104, 76; HRMS *m/z* calcd for $C_{12}H_{10}O_4$ (M^+) 218.05791, found 218.0579.] The presence of these acid-containing solids on the cold wall of the quartz tube, near the exit side, can explain the absence of the expected NH_3 evolution as observed during the thermal degradation of the control sample of PPy powder. It is believed that most of the released NH_3 might have been absorbed by these solid acids and rendered its detection impossible.

Apparently, all the above solid byproducts were yielded from the thermal degradation of PET core fiber, as no detectable solid byproducts (e.g. oligomeric pyrroles) from the thermal degradation of PPy skin layer were found in the sublimed compounds. Such findings are consistent with the observation that the polypyrrole skin is thermally much more stable than the PET core and thus confirm that the walls of the carbon tubes were mainly derived from the PPy skin layer.

Conclusions

The formation mechanisms of micrometer-sized carbon tubes and the corresponding PPy/PET composite fibers have been studied in this report with various

spectroscopic methods. The investigations indicated that the morphological quality, integrity, and thickness of the PPy coating layer are the most crucial properties in determining the success of obtaining hollow and opened carbon tube structures. The PPy/PET composite fibers produced from the multiple coating cycles were all capable of forming carbon tubes, whereas those obtained from the first coating cycle were not. The different tube formation behaviors of these composite fibers may very likely be attributed to the morphological difference between PPy layers from the first coating cycle and subsequent coating cycles. SEM investigations suggested that the formation mechanism and coating morphology for the PPy layer yielded from the first coating cycle might have been very different from those produced from subsequent coating cycles. The PPy layer of the first coating cycle may be mostly formed from the growth of PPy powders that were grown originally in the solution phase but chemisorbed and/or physical adsorbed on the PET fiber surface, thus resulting in a mechanically weak and poorly adhered coating layer. Whereas, those PPy coating layers from subsequent coating cycles may utilize the already deposited PPy particles (or nodules) as the growing templates and also as the nucleation centers for forming the highly intercalated PPy network-film-like layers with stronger mechanical strength. SEM observations on samples with different thermal treatments indicated that the core of composite fiber started to melt between 230 and 290 °C and then decomposed and disappeared mostly at ca. 390 °C, leaving behind only the hollow tubes. Both the diameter and wall thickness of such hollow tubes decreased continuously as the treatment temperature was increased, during the subsequent carbonization stage. The results herein also indicated that the gaseous byproducts originated from the PET core fiber, such as CO, CO_2, H_2O, ethene, ethanal, and acetylene, were all evolved below 500 °C, whereas the gaseous byproducts from the PPy skin layer, such as HCN, NH_3, and N_2, was mainly evolved at temperatures higher than 500 °C. The sublimed solid byproducts, formed mostly between 350 and 450 °C, were found to be mainly terephthalic acid together with some small amounts of 4-(vinyloxycarbonyl)benzoic acid and bis(vinyloxycarbonyl)benzene, which were all originated from the core PET, possibly due to backbone scission via β-hydrogen elimination.[15] [The sublimation point for terephthalic acid is 402 °C (*Merck Index*, 12th ed.; Merck & Co., Inc.: Rahway, NJ, 1996). The initial and the onset temperatures for the sublimation of 4-(vinyloxycarbonyl)benzoic acid, measured by TG-DTA, were 110 and 171 °C, respectively; while the initial and the onset temperatures for the sublimation of 1,4-bis(vinyloxycarbonyl)benzene were 84 and 154 °C, respectively.] However, none of the gaseous or solid byproducts released below 1000 °C were found to associate with the PPy backbone scission. These results are consistent with the general understanding and observation that PPy is thermally more stable than PET and, thus, confirm that the walls of the carbon tubes were mainly derived from the PPy skin layers.

Acknowledgment. We acknowledge financial support from the National Science Council of ROC and Chinese Petroleum Corp.

CM010141F